Bioorganic & Medicinal Chemistry 19 (2011) 1464–1470

Contents lists available at ScienceDirect

Bioorganic & Medicinal Chemistry

journal homepage: www.elsevier.com/locate/bmc

Practical synthesis of precursor of [*N-methyl*-^{11}C]vorozole, an efficient PET tracer targeting aromatase in the brain

Kayo Takahashi [a], Gen Yamagishi [b], Toshiyuki Hiramatsu [b,c], Ayako Hosoya [b,c], Kayo Onoe [a], Hisashi Doi [a], Hiroko Nagata [a], Yasuhiro Wada [a], Hirotaka Onoe [a], Yasuyoshi Watanabe [a], Takamitsu Hosoya [b,c,*]

[a] *RIKEN Center for Molecular Imaging Science, 6-7-3 Minatojima-minamimachi, Chuo-ku, Kobe 650-0047, Japan*
[b] *Department of Biological Information, Graduate School of Bioscience and Biotechnology, Tokyo Institute of Technology, 4259 Nagatsuta-cho, Midori-ku, Yokohama 226-8501, Japan*
[c] *Laboratory of Chemical Biology, Graduate School of Biomedical Science, Institute of Biomaterials and Bioengineering, Tokyo Medical and Dental University, 2-3-10 Kanda-Surugadai, Chiyoda-ku, Tokyo 101-0062, Japan*

ARTICLE INFO

Article history:
Received 10 December 2010
Revised 27 December 2010
Accepted 28 December 2010
Available online 1 January 2011

Keywords:
Aromatase inhibitor
Vorozole
Positron emission tomography (PET)
Carbon-11

ABSTRACT

A practical method to prepare precursor of [*N-methyl*-^{11}C]vorozole ([^{11}C]vorozole), an efficient positron emission tomography (PET) tracer for imaging aromatase in the living body, was established. Sufficient amount of the racemate including norvorozole, a demethylated vorozole derivative used as a precursor of [^{11}C]vorozole, became available by means of high-yield eight-step synthesis. The enantiomers were separated by preparative HPLC using a chiral stationary phase column to give optically pure norvorozole and its enantiomer. From the latter, *ent*-[^{11}C]vorozole, an enantiomer of [^{11}C]vorozole, was prepared and used in the PET study for the first time, which was shown to bind very weakly to aromatase in rhesus monkey brain supporting the previous pharmacological results. The stable supply of norvorozole will facilitate further researches on aromatase in the living body including brain by the PET technique.

1. Introduction

Aromatase, one of the monooxygenase families of enzymes,[1] catalyzes the biosynthetic conversion of androgens to estrogens.[2,3] It consists of a specific aromatase cytochrome P450, the CYP19 gene product, and the flavoprotein NADPH-cytochrome P450 reductase. Aromatase has a single binding site for the substrates in the highly conserved heme domain of the enzyme.[4] The recent X-ray structural study using native aromatase purified from human placenta clearly showed that the substrates fit tightly in the androgen-specific cleft, in which the aromatization takes place.[5] This makes a sharp contrast with many other microsomal P450s, which can recognize and metabolize various structurally-diverse drugs and xenobiotics owing to their flexible active sites.

In humans, aromatase is expressed in a wide variety of tissues such as placenta, ovary, adipose tissue, skin, central nervous system, hair follicles, testicle, liver, and muscle.[2,4] Abundant amount of aromatase is expressed in the ovary, which is the major source of circulating estrogens in premenopausal women. Though, after menopause, the ovary ceases to produce estrogens, aromatase continues to synthesize estrogens in the non-ovarian tissues,[6] including the breast tissue.[7] Approximately two thirds of postmenopausal breast cancer patients have estrogen-dependent cancer,[8] that is, estrogen can stimulate tumor growth by binding to its receptor, which is expressed in the tumor cells. Furthermore, 63–72% of breast cancer cells possess aromatase activity,[9] which triggers the local synthesis of estrogen promoting the tumor growth. Hence, aromatase is one of the most common target proteins in the treatment of hormone-dependent breast cancer. Indeed, several aromatase inhibitors have been used clinically for the treatment of breast cancer in postmenopausal patients.[8,10]

Aromatase inhibitors can be categorized into two general types based on their structural feature, namely steroidal and non-steroidal inhibitors (Fig. 1).[8,10] Exemestane (**1**, Aromasin™), structurally similar to endogenous androgens, is a representative steroidal inhibitor, which binds irreversibly to the enzyme and inactivates it.[11] In contrast, the non-steroidal inhibitors such as anastrozole (**2**, Arimidex™)[12] and letrozole (**3**, Femara™),[13] competitively inhibit the enzymatic activity of aromatase in a

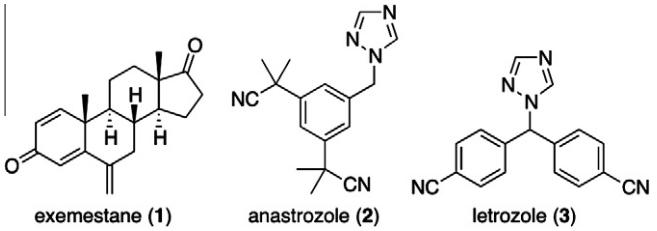

Figure 1. Clinically-used aromatase inhibitors.

* Corresponding author. Tel./fax: +81 3 5280 8117.
E-mail address: thosoya.cb@tmd.ac.jp (T. Hosoya).

0968-0896/$ - see front matter © 2010 Elsevier Ltd. All rights reserved.
doi:10.1016/j.bmc.2010.12.057

reversible manner. The triazole moiety of these drugs has been considered to coordinate to the iron atom that resides in the heme domain of the enzyme showing highly selective inhibitory activity toward aromatase.[14] These three drugs are included in the third-generation aromatase inhibitors and have been evaluated clinically.[15]

Expression of aromatase is detected not only in the peripheral systems, but also in the brain, in which its functions have been attracting much attention.[16] It has been considered that aromatase in the brain is related to reproductive behaviors and sexual differentiation of the brain.[16a] Recently, it has been suggested to be involved in neuroprotection[16b,c] as well as emotional behaviors.[17] Although most of the studies of detecting aromatase proteins in tissues had been performed by immunohistochemistry and Western blot and Northern blot analyses, these techniques are inadequate to survey the dynamic functions of aromatase in the living body including the brain. In fact, the relationships between the aromatase enzymatic activity and its diverse functions in the brain are not fully understood.

In order to study aromatase expressed in the living body, positron emission tomography (PET) technique, a noninvasive in vivo molecular imaging method, has been introduced.[18] In the PET study, a PET tracer labeled with a short-lived positron-emitting radionuclide such as ^{11}C and ^{18}F with a half-life period of 20 and 110 min, respectively, is employed. So far, some PET tracers with potent aromatase inhibitory activity including [*N-methyl*-^{11}C]vorozole ([^{11}C]vorozole, (*S*)-[^{11}C]-**4**) (Fig. 2),[19] ^{11}C-labeled sulfonanilide analogs,[20] ^{11}C-labeled sulfamate derivatives (dual aromatase–steroid sulfatase inhibitors),[21] and [*cyano*-^{11}C]letrozole,[22] have been developed.

Vorozole ((*S*)-**4**) is a potent and specific non-steroidal aromatase inhibitor, which was developed to treat breast cancer.[23] It shares a common triazole substructure with anastrozole (**2**) and letrozole (**3**) showing higher inhibitory activity toward aromatase than these clinically-used drugs.[24] Since vorozole has a methyl group, which is covalently bound to one of the nitrogen atom on the benzotriazole ring, [^{11}C]vorozole has been prepared easily by S_N2-type *N*-[^{11}C]methylation of norvorozole ((*S*)-**5**), a demethyl derivative of vorozole, treating it with [^{11}C]H_3I under basic conditions.[19] Recently, it was pointed out that all of three possible N-methylations proceed by this reaction and careful separation of [^{11}C]vorozole ((*S*)-[^{11}C]-**4**) from the inactive isomers should be taken into account to obtain reliable PET images.[25] By using [^{11}C]vorozole as a PET tracer, the localization of aromatase on the amygdala and hypothalamus in living rhesus monkey brain was discovered,[26a] and increased aromatase level in the hypothalamic region of rats evoked by treatment of anabolic-androgenic steroids was observed as well.[26b,c] Recent PET study using [^{11}C]vorozole in human brain has revealed unique distribution of aromatase in thalamus and medulla.[27]

Despite the utility of [^{11}C]vorozole in PET studies, its precursor, norvorozole ((*S*)-**5**), is not easily available. At present, it almost entirely depends on donation from the pharmaceutical company and its detailed synthetic procedure has not been appeared in any of the literatures including patents. With the aim of promoting the PET study of aromatase in the brain, we examined to establish a practical preparative method of norvorozole ((*S*)-**5**). Herein we describe the synthetic route of racemic mixture of norvorozole ((*S*)-**5**) and its enantiomer as well as the conditions of their optical resolution. The results of PET studies comparing the binding of [^{11}C]vorozole and its enantiomer toward aromatase in rhesus monkey brain are also noted.

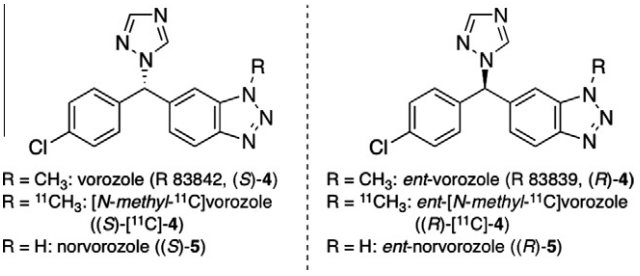

Figure 2. Structures of vorozole, [*N-methyl*-^{11}C]vorozole, norvorozole, and their enantiomers.

2. Results and discussion

2.1. Synthesis and optical resolution of racemic mixture of norvorozole and its enantiomer

At the early phase of the drug development, the biological activities of vorozole ((*S*)-**4**) were evaluated as a racemic mixture with its enantiomer, which was referred to as R 76713 (*rac*-**4**) (Fig. 2).[28a] Afterward, the (+)-(*S*)-isomer, R 83842, and its enantiomer, R 83839 (*ent*-vorozole, (*R*)-**4**), were prepared in an optically pure form and the former isomer with more potent bioactivities was referred to as vorozole ((*S*)-**4**).[20,23,28] Indeed, the IC_{50} values of vorozole ((*S*)-**4**) and *ent*-vorozole ((*R*)-**4**) toward aromatase in rat granulosa cells were reported as 0.44 and 240 nM, respectively, showing more than 500-fold difference in potency between the enantiomers.[28c] The K_i value of vorozole ((*S*)-**4**) against human placental aromatase was 0.7 nM, which was also 25-times more potent than *ent*-vorozole.[28c] Therefore, the clinical studies were focused on the more potent enantiomer, vorozole ((*S*)-**4**).

Vorozole ((*S*)-**4**), in an optically pure form, was prepared from an optically pure synthetic intermediate, which was obtained by selective crystallization of diasteromeric salts of hydrazine derivative and a chiral acid.[29] This optical resolution procedure was optimized to obtain vorozole ((*S*)-**4**) and preparation of no other related compounds in optically pure form including norvorozole ((*S*)-**5**) were reported. In principle, norvorozole ((*S*)-**5**) can be obtained directly from vorozole ((*S*)-**4**) by removing its *N*-methyl group. In usual, however, it is not easy to remove *N*-methyl group under mild condition without racemization. Moreover, preparing optically pure norvorozole ((*S*)-**5**) by the method mentioned above for vorozole ((*S*)-**4**) seemed unsuitable because *N*-methyl group was introduced at the early stage of the synthesis.[29] Thus, we decided to establish a new synthetic route, which is appropriate to obtain sufficient amount of norvorozole ((*S*)-**5**).

In order to prepare norvorozole ((*S*)-**5**) in a practical manner, we chose to synthesize the racemate first and separate the enantiomers by preparative HPLC using a chiral stationary phase column. We also decided to construct the benzotriazole unit at the final step to avoid the unnecessary difficulties for structural analysis of intermediate compounds, which would arise from the formation of benzotriazole isomers. Based on these ideas, we finally succeeded in developing a practical preparative method of norvorozole ((*S*)-**5**) and its enantiomer *ent*-norvorozole ((*R*)-**5**) as summarized in Scheme 1.

We selected commercially available 4,4′-dichloro-3-nitrobenzophenone (**6**) as the starting material. At first, one of the two chloro groups attached on the more electron deficient benzene ring was selectively displaced by an azido group to give **7**. Subsequent catalytic hydrogenation of **7** led to reduction of azido and nitro groups at once to give *o*-phenylenediamine derivative **8**. The protection of the both amino groups of **8** by Boc group followed by sodium borohydride reduction gave benzhydrol derivative **10**. Treatment of alcohol **10** with mesyl chloride in the presence of triethylamine afforded a mixture of corresponding mesylate **11** and chloride **12**, which was produced by chlorination of **11**. Since both compounds could be used in the next step equally, we did not optimize the

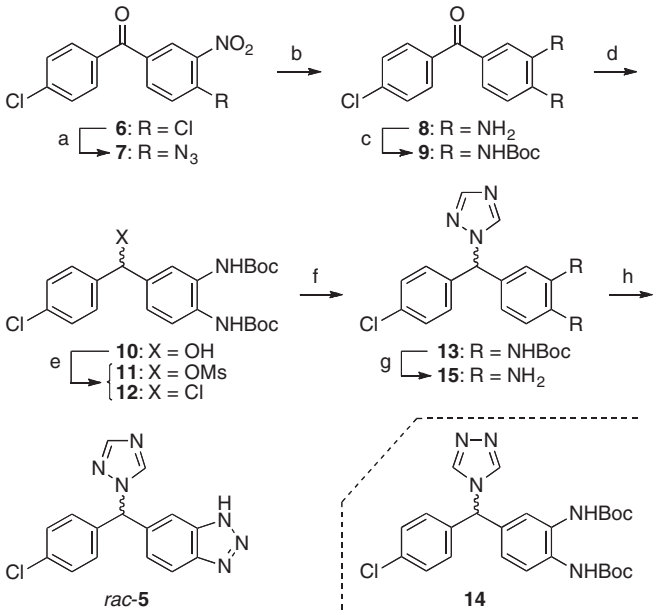

Scheme 1. Synthesis of racemic mixture of norvorozole and its enantiomer. Reagents and conditions: (a) NaN_3, DMF, 0 °C to room temperature, 2 h, 98%; (b) H_2, 10% Pd–C, THF, room temperature, 15 h, 82%; (c) Boc_2O, iPr_2NEt, reflux, 24 h, 44%; (d) $NaBH_4$, THF–EtOH (1:1, v/v), 0 °C to room temperature, 2 h, quant.; (e) CH_3SO_2Cl, Et_3N, THF–CH_2Cl_2 (1:1, v/v), 0 °C to room temperature, 4 h; (f) 1,2,4-triazole, K_2CO_3, acetone, room temperature, 16 h, 69% of **13** (two-steps) and 15% of **14** (two-steps); (g) TFA, CH_2Cl_2, 0 °C, 4 h, 85%; (h) $NaNO_2$, aq HCl, 0 °C, 1 h, 93%.

reaction conditions any more and the mixture was used without further purification. Thus, the mixture of **11** and **12** was reacted with 1,2,4-triazole under basic conditions to form approximately 5:1 mixture of desired triazole derivative **13** and its regioisomer **14**, which were easily separated by chromatography. After deprotection of Boc groups of **13** by TFA, the resulting diamine **15** was treated with sodium nitrite under acidic conditions to construct the benzotriazole unit affording *rac*-**5**, a racemic mixture of norvorozole ((*S*)-**5**) and its enantiomer, *ent*-norvorozole ((*R*)-**5**). The TLC behavior and ^1H NMR spectrum of the synthetic sample matched exactly with those of the authentic sample. It took only eight simple reaction steps in approximately 20% overall yield to prepare *rac*-**5** from the starting material, showing the practicality of the synthetic route.

Next, we examined to separate the enantiomers of *rac*-**5** by preparative HPLC using a chiral stationary phase column. After some efforts to screen separating conditions including column types, combination and composition of solvents for mobile phase, we found the practical conditions. Consequently, using CHIRALPAK AD-H column (Daicel Chemical) eluting with EtOH/MeOH (7:3, v/v) was effective to obtain both norvorozole ((*S*)-**5**) and its enantiomer *ent*-norvorozole ((*R*)-**5**) in optically pure forms (Supplementary Fig. 1). The isomer that eluted later was unambiguously determined as norvorozole ((*S*)-**5**) by comparing it with the authentic sample.

2.2. PET imaging using [^{11}C]vorozole and *ent*-[^{11}C]vorozole in the rhesus monkey brain

With both norvorozole ((*S*)-**5**) and *ent*-norvorozole ((*R*)-**5**) in hand, we were interested in comparing the brain distribution of [^{11}C]vorozole ((*S*)-[^{11}C]-**4**) and its enantiomer, *ent*-[^{11}C]vorozole ((*R*)-[^{11}C]-**4**). Thus, both PET tracers were synthesized and carefully purified according to the modified method reported recently.[25]

The prepared PET tracer, [^{11}C]vorozole ((*S*)-[^{11}C]-**4**) or *ent*-[^{11}C]vorozole ((*R*)-[^{11}C]-**4**), were intravenously administered to anesthetized rhesus monkeys and their brain was scanned by a PET camera. The distribution volume ratio (DVR) images obtained for horizontal and coronal sections are shown in Figure 3, in which the binding potential of each tracer to brain aromatase are represented. Consequently, a high DVR of [^{11}C]vorozole ((*S*)-[^{11}C]-**4**) was observed in the amygdala and hypothalamus which was consistent with the previous study.[26a] On the contrary, relatively low DVR of *ent*-[^{11}C]vorozole ((*R*)-[^{11}C]-**4**) was detected throughout the brain.

Based on the results of PET images, the time–activity curves of PET tracers were obtained. As employed in the previous study,[26a] the cerebellum region was selected as a reference region, which was regarded not to contain aromatase enzyme. Thus, the normalized time–activity curves of [^{11}C]vorozole ((*S*)-[^{11}C]-**4**) and *ent*-[^{11}C]vorozole ((*R*)-[^{11}C]-**4**) in the aromatase-rich regions, the amygdala and hypothalamus, were generated by dividing by that of the cerebellum region (Fig. 4). As a result, the normalized SUVs (standardized uptake values), the ratios of aromatase-rich regions to the reference region, of [^{11}C]vorozole ((*S*)-[^{11}C]-**4**), were higher than 1.0 throughout the monitoring time, while that of *ent*-[^{11}C]vorozole ((*R*)-[^{11}C]-**4**) were close to 1.0, indicating that [^{11}C]vorozole ((*S*)-[^{11}C]-**4**) binds to aromatase more specifically, but *ent*-[^{11}C]vorozole ((*R*)-[^{11}C]-**4**) does not.

DVR images and normalized time–activity curves indicated that the binding of *ent*-[^{11}C]vorozole ((*R*)-[^{11}C]-**4**) in the amygdala and hypothalamus is less specific than that of [^{11}C]vorozole ((*S*)-[^{11}C]-**4**). Our present result showing the large difference of aromatase binding between [^{11}C]vorozole ((*S*)-[^{11}C]-**4**) and *ent*-[^{11}C]vorozole ((*R*)-[^{11}C]-**4**) was consistent with previously reported IC_{50} and K_i values for these enantiomers.[28] Furthermore, it was demonstrated that no significant epimerization of vorozole occurs in in vivo at least during the period of PET scanning. This information, in general, would be important to achieve for optically active drug candidates.

3. Conclusion

In summary, we established a practical preparative method of optically pure norvorozole ((*S*)-**5**) by means of high-yield eight-step synthesis of the racemate followed by its separation by preparative HPLC using a chiral stationary phase column. The stable supply of norvorozole ((*S*)-**5**) will facilitate further researches on aromatase in the living body by the aromatase specific PET tracer, [^{11}C]vorozole ((*S*)-[^{11}C]-**4**).

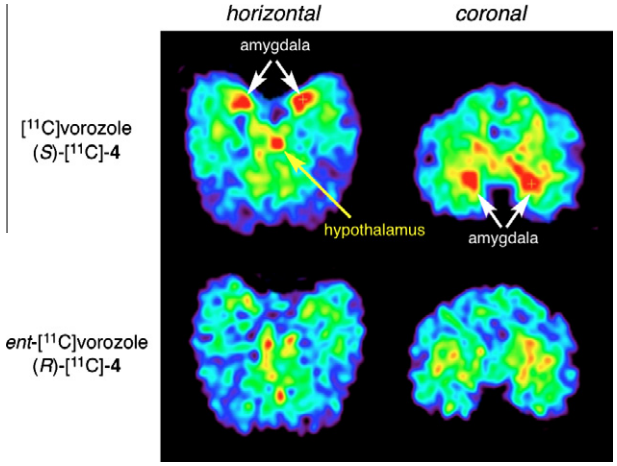

Figure 3. The distribution volume ratio (DVR) images of [^{11}C]vorozole ((*S*)-[^{11}C]-**4**) (upper panels) and *ent*-[^{11}C]vorozole ((*R*)-[^{11}C]-**4**) (lower panels) in the rhesus monkey brain. Left panels: horizontal sectional view; Right panels: coronal sectional view. White and yellow arrows indicate amygdala and hypothalamus, respectively.

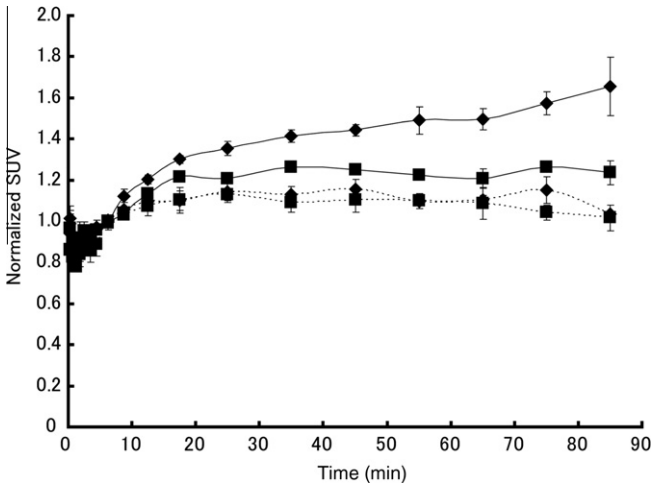

Figure 4. The normalized time–activity curves of [^{11}C]vorozole ((*S*)-[^{11}C]-**4**) (solid line) and *ent*-[^{11}C]vorozole ((*R*)-[^{11}C]-**4**) (dashed line) at aromatase-rich regions, the amygdala (filled rhombus) and hypothalamus (filled square), in the rhesus monkey brain. SUV (standardized uptake value) represents as (radioactivity in tissue/volume of tissue)/(injected radioactivity/body weight).

4. Experimental

4.1. Chemistry

General: All chemical reagents used were commercial grade and used as received. Analytical thin-layer chromatography (TLC) was performed on precoated (0.25 mm) silica-gel plates (Merck Chemicals, Silica Gel 60 F_{254}). Column chromatography was conducted using silica-gel (Kanto Chemical Co., Inc., Silica Gel 60N, spherical neutral, particle size 40–50 μm or 63–210 μm). The optical resolution of racemic compound was performed by preparative HPLC using a chiral stationary phase column CHIRALPAK AD-H (20 mm i.d. × 250 mm, attached with a guard column; 10 mm i.d. × 20 mm, Daicel Chemical Ind., Ltd, Japan). The optical purity of separated compounds was determined by analytical HPLC using a chiral stationary phase column CHIRALPAK AD-H (4.6 mm i.d. × 250 mm, attached with a guard column; 4.0 mm i.d. × 10 mm, Daicel Chemical Ind., Ltd, Japan). Specific optical rotation ($[\alpha]_D$) was measured on a JASCO DIP-370 digital polarimeter. ^{1}H and ^{13}C NMR spectra were obtained with a Varian MERCURY 300 spectrometer at 300 and 75.5 MHz, respectively. $CDCl_3$ (CIL) and DMSO-d_6 (CIL) were used as solvents for obtaining NMR spectra. Chemical shifts (δ) are given in parts per million (ppm) downfield from $(CH_3)_4Si$ (δ 0.00 for ^{1}H NMR in $CDCl_3$) or the solvent peak (δ 2.49 for ^{1}H NMR and δ 39.5 for ^{13}C NMR in DMSO-d_6, and δ 77.0 for ^{13}C NMR in $CDCl_3$) as an internal reference with coupling constants (*J*) in hertz (Hz). The abbreviations s, d, m, and br signify singlet, doublet, multiplet, and broad, respectively. IR spectra were measured by diffuse reflectance method on a SHIMADZU IRPrestige-21 spectrometer attached with DRS-8000A with the absorption band given in cm^{-1}. High-resolution mass spectra (HRMS) were measured on a JEOL JMS-700 mass spectrometer under or electron impact ionization (EI) condition or positive fast atom bombardment (FAB$^+$) condition using *m*-nitrobenzyl alcohol (NBA) as a matrix at the Center for Advanced Materials Analysis (Suzukakedai), Technical Department, Tokyo Institute of Technology.

4.1.1. 4-Azido-4′-chloro-3-nitrobenzophenone (7)

To a solution of 4,4′-dichloro-3-nitrobenzophenone (**6**, Sigma–Aldrich) (17.5 g, 59.1 mmol) in DMF (60 mL) was added sodium azide (4.61 g, 70.9 mmol) at 0 °C. The mixture was warmed to room temperature and stirred for 2 h. To this was added water (300 mL) and the mixture was extracted with EtOAc (150 mL × 3). The combined organic extracts were successively washed with water (100 mL × 3) and brine (100 mL × 1), dried over Na_2SO_4, filtered, and concentrated under reduced pressure. The residue was purified by column chromatography (silica-gel 220 g, *n*-hexane/EtOAc = 9:1) to give 4-azido-4′-chloro-3-nitrobenzophenone (**7**) (17.6 g, 98.4%) as a pale yellow solid; TLC R_f = 0.41 (*n*-hexane/EtOAc = 4:1); ^{1}H NMR (300 MHz, $CDCl_3$) δ 7.47 (d, 1H, *J* = 8.5 Hz, aromatic), 7.49–7.57 (AA′BB′, 2H, aromatic), 7.69–7.78 (AA′BB′, 2H, aromatic), 8.08 (dd, 1H, *J* = 2.0, 8.5 Hz, aromatic), 8.34 (d, 1H, *J* = 2.0 Hz, aromatic); ^{13}C NMR (75.5 MHz, $CDCl_3$) δ 120.8, 127.6, 129.0 (2C), 131.1 (2C), 133.4, 134.4, 134.7, 138.6, 139.7, 140.1, 191.6; IR (KBr, cm^{-1}) 687, 714, 754, 847, 876, 914, 964, 980, 1015, 1072, 1090, 1175, 1256, 1294, 1352, 1400, 1487, 1533, 1566, 1587, 1607, 1661, 2131; HRMS (EI) *m*/*z* 302.0205 (M$^+$, $C_{13}H_7{}^{35}ClN_4O_3$ required 302.0207).

4.1.2. 3,4-Diamino-4′-chlorobenzophenone (8)

Under argon atmosphere, to a solution of 4-azido-4′-chloro-3-nitrobenzophenone (**7**) (5.00 g, 16.5 mmol) in THF (80 mL) was added palladium/charcoal activated (10%) (500 mg) at room temperature. The gas in the reaction flask was evacuated and refilled with hydrogen gas. After stirring for 15 h, the internal gas was returned to argon and to the mixture was added CH_2Cl_2 (300 mL) and stirred for 30 min under air. The catalyst was removed by filtration and the filtrate was concentrated under reduced pressure. The residue was purified by column chromatography (silica-gel 220 g, CH_2Cl_2/CH_3OH = 40:1) to give 3,4-diamino-4′-chlorobenzophenone (**8**) (3.36 g, 82.4%) as a brown solid; TLC R_f = 0.35 (CH_2Cl_2/CH_3OH = 15:1); ^{1}H NMR (300 MHz, DMSO-d_6) δ 4.73 (s, 2H, NH_2), 5.54 (s, 2H, NH_2), 6.52 (dd, 1H, *J* = 1.4, 1.8 Hz, aromatic), 6.87 (dd, 1H, *J* = 1.8, 8.1 Hz, aromatic), 7.03 (dd, 1H, *J* = 1.4, 8.1 Hz, aromatic), 7.50–7.56 (AA′BB′, 2H, aromatic), 7.56–7.62 (AA′BB′, 2H, aromatic); ^{13}C NMR (75.5 MHz, DMSO-d_6) δ 112.3, 115.4, 122.9, 124.9, 128.2 (2C), 130.8 (2C), 134.0, 135.8, 138.3, 141.6, 192.9; IR (KBr, cm^{-1}) 758, 818, 845, 870, 905, 1090, 1142, 1161, 1292, 1325, 1396, 1449, 1518, 1558, 1587, 1612, 3370, 3435; HRMS (FAB$^+$/NBA+KCl) *m*/*z* 285.0204 ([M+K]$^+$, $C_{13}H_{11}{}^{35}ClN_2OK$ required 285.0197).

4.1.3. 4′-Chloro-3,4-di(*tert*-butoxycarbonylamino)benzophenone (9)

Under argon atmosphere, to a solution of 3,4-diamino-4′-chlorobenzophenone (**8**) (2.86 g, 11.6 mmol) in THF (100 mL) was successively added *N*,*N*-diisopropylethylamine (4.85 mL, 27.8 mmol) and di-*tert*-butyl dicarbonate (6.40 mL, 27.9 mmol) at room temperature, and the mixture was refluxed (oil bath temperature 70 °C) for 24 h. After cooling to room temperature, to this was added 1 M aqueous HCl solution (300 mL) and the mixture was extracted with EtOAc (100 mL × 3). The combined organic extracts were successively washed with water (100 mL × 1) and brine (100 mL × 1), dried over Na_2SO_4, filtered, and concentrated under reduced pressure. The residue was purified by column chromatography (silica-gel 230 g, *n*-hexane/EtOAc = 6:1) to give 4′-chloro-3,4-di(*tert*-butoxycarbonylamino)benzophenone (**9**) (2.28 g, 44.0%) as a colorless solid; TLC R_f = 0.57 (*n*-hexane/EtOAc = 2:1); ^{1}H NMR (300 MHz, $CDCl_3$) δ 1.52 (s, 9H, $3CH_3$), 1.54 (s, 9H, $3CH_3$), 6.42–6.60 (br, 1H, NH), 7.15–7.24 (br, 1H, NH), 7.42–7.51 (AA′BB′, 2H, aromatic), 7.59 (dd, 1H, *J* = 1.9, 8.5 Hz, aromatic), 7.71–7.77 (AA′BB′, 2H, aromatic), 7.80 (d, 1H, *J* = 1.9 Hz, aromatic), 7.90 (d, 1H, *J* = 8.5 Hz, aromatic); ^{13}C NMR (75.5 MHz, $CDCl_3$) δ 28.11 (3C), 28.13 (3C), 81.3, 81.4, 121.4, 127.1, 127.9, 128.2, 128.5 (2C), 131.3 (2C), 132.3, 135.7, 136.3, 138.6, 152.9, 154.1, 194.0; IR (KBr, cm^{-1}) 737, 758, 1049, 1090, 1157, 1242, 1314, 1368, 1393, 1420, 1526, 1587, 1647, 1701, 1730, 2978, 3310; HRMS (FAB$^+$/NBA+NaI) *m*/*z* 469.1508 ([M+Na]$^+$, $C_{23}H_{27}{}^{35}ClN_2O_5Na$ required 469.1506).

4.1.4. 4′-Chloro-3,4-di(*tert*-butoxycarbonylamino)benzhydrol (10)

Under argon atmosphere, to a solution of 4′-chloro-3,4-di(*tert*-butoxycarbonylamino)benzophenone (**9**) (3.00 g, 6.71 mmol) in a 1:1 mixture of THF–EtOH (60 mL) was added sodium borohydride (254 mg, 6.71 mmol) at 0 °C. The mixture was allowed to warm to room temperature and stirred for 2 h. To this was added water (200 mL) and the mixture was extracted with EtOAc (150 mL × 3). The combined organic extracts were successively washed with water (100 mL × 1) and brine (100 mL × 1), dried over Na_2SO_4, filtered, and concentrated under reduced pressure. The residue was purified by column chromatography (silica-gel 120 g, *n*-hexane/EtOAc = 2:1) to give 4′-chloro-3,4-di(*tert*-butoxycarbonylamino)benzhydrol (**10**) (3.22 g, quant.) as a colorless solid; TLC R_f = 0.36 (*n*-hexane/EtOAc = 2:1); ^{1}H NMR (300 MHz, $CDCl_3$) δ 1.499 (s, 9H, $3CH_3$), 1.504 (s, 9H, $3CH_3$), 2.57 (d, 1H, J = 3.4 Hz, OH), 5.75 (d, 1H, J = 3.4 Hz, CH), 6.65–6.84 (br, 2H, 2NH), 7.06 (dd, 1H, J = 1.9, 8.2 Hz, aromatic), 7.27–7.31 (AA′BB′, 4H, aromatic), 7.43 (d, 1H, J = 8.2 Hz, aromatic), 7.47 (d, 1H, J = 1.9 Hz, aromatic); ^{13}C NMR (75.5 MHz, $CDCl_3$) δ 28.2 (6C), 74.6, 80.8, 80.9, 122.4, 123.5, 124.2, 127.8 (2C), 128.3 (2C), 129.4, 130.0, 132.8, 140.8, 142.0, 154.0 (2C); IR (KBr, cm^{-1}) 737, 770, 818, 1015, 1026, 1049, 1090, 1157, 1248, 1368, 1393, 1491, 1524, 1597, 1697, 2978, 3329; HRMS (FAB$^+$/NBA+NaI) m/z 471.1674 ([M+Na]$^+$, $C_{23}H_{29}{}^{35}ClN_2O_5Na$ required 471.1663).

4.1.5. 4-{(4-Chlorophenyl)(1*H*-1,2,4-triazol-1-yl)methyl}-1,2-di(*tert*-butoxycarbonylamino)benzene (13)

Under argon atmosphere, to a solution of 4′-chloro-3,4-di(*tert*-butoxycarbonylamino)benzhydrol (**10**) (1.50 g, 3.34 mmol) in a 1:1 mixture of THF–CH_2Cl_2 (28 mL) was successively added triethylamine (700 μL, 5.02 mmol) and methanesulfonyl chloride (310 μL, 4.01 mmol) at 0 °C. The mixture was allowed to warm to room temperature and stirred for 4 h. This was poured into water (100 mL) and the mixture was extracted with CH_2Cl_2 (100 mL × 3). The combined organic extracts were washed with brine (100 mL × 1), dried over Na_2SO_4, filtered, and concentrated under reduced pressure to give a crude mixture of 4-{chloro(4-chlorophenyl)methyl}-1,2-di(*tert*-butoxycarbonylamino)benzene (**11**) and {3,4-bis(*tert*-butoxycarbonylamino)phenyl}(4-chlorophenyl)methyl methanesulfonate (**12**) (2.02 g) as a colorless oil.

Under argon atmosphere, to a solution of the crude product obtained as above in acetone (30 mL) was successively added potassium carbonate (1.38 g, 10.0 mmol) and 1,2,4-triazole (461 mg, 6.68 mmol) at room temperature. After stirring for 16 h at the same temperature, the mixture was filtered and the filtrate was concentrated under reduced pressure. The residue was purified by column chromatography (silica-gel 120 g, *n*-hexane/EtOAc = 3:2–2:3) to give 4-{(4-chlorophenyl)(1*H*-1,2,4-triazol-1-yl)methyl}-1,2-di(*tert*-butoxycarbonylamino)benzene (**13**) (1.16 g, 68.8%, two-step yield based on **10**) as a colorless solid; TLC R_f = 0.50 (*n*-hexane/EtOAc = 1:1); ^{1}H NMR (300 MHz, $CDCl_3$) δ 1.49 (s, 9H, $3CH_3$), 1.51 (s, 9H, $3CH_3$), 6.67 (s, 1H, CH), 6.72 (br s, 1H, NH), 6.83 (br s, 1H, NH), 6.90 (dd, 1H, J = 2.0, 8.7 Hz, aromatic), 7.00–7.10 (AA′BB′, 2H, aromatic), 7.27–7.40 (m, 3H, aromatic), 7.56 (d, 1H, J = 8.7 Hz, aromatic), 7.97 (s, 1H, aromatic), 8.02 (s, 1H, aromatic); ^{13}C NMR (75.5 MHz, $CDCl_3$) δ 27.9 (6C), 66.1, 80.4, 80.5, 123.3, 123.7, 124.1, 128.6 (2C), 129.0 (2C), 130.1, 130.4, 133.1, 134.0, 136.2, 143.2, 151.7, 153.4 (2C); IR (KBr, cm^{-1}) 660, 679, 737, 787, 1015, 1049, 1091, 1157, 1244, 1368, 1493, 1526, 1597, 1709, 2978, 3308; HRMS (FAB$^+$/NBA+NaI) m/z 522.1900 ([M+Na]$^+$, $C_{25}H_{30}{}^{35}ClN_5O_4Na$ required 522.1884).

Further elution with EtOAc also gave the isomer 4-{(4-chlorophenyl)(4*H*-1,2,4-triazol-4-yl)methyl}-1,2-di(*tert*-butoxycarbonylamino)benzene (**14**) (248 mg, 14.8%, two-step yield based on **10**) as a colorless solid; TLC R_f = 0.50 (EtOAc only), R_f = 0.12 (*n*-hexane/EtOAc = 1:1); ^{1}H NMR (300 MHz, $CDCl_3$) δ 1.49 (s, 9H, $3CH_3$), 1.52 (s, 9H, $3CH_3$), 6.50 (s, 1H, CH), 6.75–6.88 (m, 2H, aromatic), 7.00–7.10 (AA′BB′, 2H, aromatic), 7.30–7.43 (m, 3H, aromatic and 2NH), 7.55 (d, 1H, J = 8.0 Hz, aromatic), 8.04 (s, 2H, aromatic); ^{13}C NMR (75.5 MHz, $CDCl_3$) δ 28.1 (6C), 62.6, 81.15, 81.20, 123.4, 124.0, 124.8, 129.1 (2C), 129.4 (2C), 131.0, 133.4, 135.0, 135.9, 142.6 (2C), 146.6, 153.7 (2C); IR (KBr, cm^{-1}) 650, 737, 783, 1015, 1024, 1051, 1091, 1157, 1246, 1308, 1368, 1491, 1522, 1708, 2978, 3294; HRMS (FAB$^+$/NBA+NaI) m/z 522.1878 ([M+Na]$^+$, $C_{25}H_{30}{}^{35}ClN_5O_4Na$ required 522.1884).

4.1.6. 1,2-Diamino-4-{(4-chlorophenyl)(1*H*-1,2,4-triazol-1-yl)-methyl}benzene (15)

Under argon atmosphere, to a solution of 4-{(4-chlorophenyl)(1*H*-1,2,4-triazol-1-yl)methyl}-1,2-di(*tert*-butoxycarbonylamino)benzene (**13**) (1.00 g, 2.00 mmol) in CH_2Cl_2 (2.0 mL) was added trifluoroacetic acid (2.0 mL) at 0 °C. After stirring at the same temperature for 4 h, to this was added saturated aqueous $NaHCO_3$ solution (100 mL) and the mixture was extracted with CH_2Cl_2 (50 mL × 3). The combined organic extracts were dried over Na_2SO_4, filtered, and concentrated under reduced pressure. The residue was purified by column chromatography (silica-gel 120 g, EtOAc only to EtOAc/CH_3OH = 15:1) to give 1,2-diamino-4-{(4-chlorophenyl)(1*H*-1,2,4-triazol-1-yl)methyl}benzene (**15**) (511 mg, 85.2%) as a colorless solid; TLC R_f = 0.41 (EtOAc only); ^{1}H NMR (300 MHz, DMSO-d_6) δ 4.48–4.55 (br, 4H, $2NH_2$), 6.24 (dd, 1H, J = 1.9, 8.0 Hz, aromatic), 6.41 (d, 1H, J = 1.9 Hz, aromatic), 6.47 (d, 1H, J = 8.0 Hz, aromatic), 6.75 (s, 1H, CH), 7.13–7.16 (AA′BB′, 2H, aromatic), 7.39–7.41 (AA′BB′, 2H, aromatic), 8.03 (s, 1H, aromatic), 8.42 (s, 1H, aromatic); ^{13}C NMR (75.5 MHz, DMSO-d_6) δ 65.4, 113.9, 114.0, 117.2, 126.7, 128.3 (2C), 129.5 (2C), 132.2, 135.0, 135.1, 139.1, 144.0, 151.7; IR (KBr, cm^{-1}) 611, 658, 679, 741, 789, 856, 961, 1015, 1090, 1136, 1202, 1275, 1296, 1406, 1445, 1491, 1518, 1593, 1626, 3345; HRMS (FAB$^+$/NBA) m/z 299.0945 (M$^+$, $C_{15}H_{14}{}^{35}ClN_5$ required 299.0938).

4.1.7. 6-{(4-Chlorophenyl)(1*H*-1,2,4-triazol-1-yl)methyl}-1*H*-benzo[*d*][1,2,3]triazole (*rac*-5)

To a solution of 1,2-diamino-4-{(4-chlorophenyl)(1*H*-1,2,4-triazol-1-yl)methyl}benzene (**14**) (460 mg, 1.53 mmol) in 0.2 M aqueous HCl (30 mL) was added sodium nitrite (111 mg, 1.61 mmol) at 0 °C. After stirring at the same temperature for 1 h, to this was added saturated aqueous $NaHCO_3$ solution (100 mL) and the mixture was extracted with EtOAc (50 mL × 3). The combined organic extracts were successively washed water (50 mL × 1) and brine (50 mL × 1), dried over Na_2SO_4, filtered, and concentrated under reduced pressure. The residue was purified by column chromatography (silica-gel 50 g, EtOAc only) to give 6-{(4-chlorophenyl)(1*H*-1,2,4-triazol-1-yl)methyl}-1*H*-benzo[*d*][1,2,3]triazole (*rac*-**5**) (444 mg, 93.1%) as a colorless solid; TLC R_f = 0.48 (EtOAc only); ^{1}H NMR (300 MHz, DMSO-d_6) δ 7.20–7.30 (AA′BB′, 2H, aromatic), 7.334 (s, 1H, aromatic or CH), 7.340 (d, 1H, J = 8.7 Hz, aromatic), 7.40–7.53 (AA′BB′, 2H, aromatic), 7.67 (s, 1H, aromatic or CH), 7.92 (d, 1H, J = 8.7 Hz, aromatic), 8.11 (d, 1H, J = 1.7 Hz, aromatic), 8.67 (d, 1H, J = 1.7 Hz, aromatic), 15.6–16.0 (br, 1H, NH); ^{13}C NMR (75.5 MHz, DMSO-d_6) δ 64.1, 114.3, 115.6, 125.8, 128.7 (2C), 130.0 (2C), 132.9, 136.3, 137.9, 138.6, 144.8, 152.2 (One carbon was not observed or overlapped with other peak. See ^{13}C NMR spectrum in Supplementary Fig. 2.); IR (KBr, cm^{-1}) 677, 739, 777, 856, 959, 995, 1015, 1092, 1136, 1206, 1275, 1410, 1437, 1491, 1636, 3372; HRMS (FAB$^+$/NBA) m/z 311.0809 ([M+H]$^+$, $C_{15}H_{12}{}^{35}ClN_6$ required 311.0812).

4.1.8. (*S*)-6-((4-Chlorophenyl)(1*H*-1,2,4-triazol-1-yl)methyl)-1*H*-benzo[*d*][1,2,3]triazole (norvorozole, (*S*)-5) and (*R*)-6-((4-chlorophenyl)(1*H*-1,2,4-triazol-1-yl)methyl)-1*H*-benzo[*d*][1,2,3]-triazole (*ent*-norvorozole, (*R*)-5)

The racemic mixture *rac*-**5** was separated to optically pure (*S*)-**5** and (*R*)-**5** by preparative HPLC using CHIRALPAK AD-H: mobile phase, EtOH/MeOH = 70:30 (v/v); flow rate, 3.0 mL/min; detection, UV at 254 nm. After concentration of each collected fraction under reduced pressure, the residue was redissolved in H_2O/MeOH and lyophilized to give a colorless solid. The enantiomeric excess (ee) of both of separated compounds was determined to be >99% by analytical HPLC using CHIRALPAK AD-H: mobile phase, EtOH/MeOH = 70:30 (v/v); flow rate, 1.0 mL/min; detection, UV at 254 nm; retention time, (*S*)-**5**: 6.8 min, (*R*)-**5**: 4.5 min (see analytical HPLC charts for *rac*-**5**, (*S*)-**5**, and (*R*)-**5** in Supplementary Fig. 1); specific optical rotation, (*S*)-**5**: $[\alpha]_D^{26}$ +24.0° (*c* 1.0 in $CHCl_3$), (*R*)-**5**: $[\alpha]_D^{26}$ −24.0° (*c* 1.0 in $CHCl_3$).

4.2. PET chemistry

General: Carbon-11 was produced by a $^{14}N(p,\alpha)^{11}C$ nuclear reaction by using a CYPRISHM-12S Cyclotron (Sumitomo Heavy Industry, Tokyo, Japan). An original automated radiolabeling system consisting of the heating of the reaction mixture, dilution, HPLC injection, fractional collection, evaporation, and sterile filtration was used for the production of $[^{11}C]H_3I$ and the ^{11}C-labeling. Purification with semi-preparative HPLC was performed on a JASCO system (Tokyo, Japan). Radioactivity was quantified with an ATOMLAB™300 dose calibrator (Aloka, Tokyo, Japan). Analytical HPLC was performed on a Shimadzu system (Kyoto, Japan) equipped with pumps and a UV detector, and the effluent radioactivity was determined by using a RLC700 radio analyzer (Aloka). The columns used for the analytical and semi-preparative HPLC were COSMOSIL C_{18} AR-II and cholester (Nacalai Tesque). $[^{11}C]H_3I$ was prepared as previously described.[30]

4.2.1. Synthesis of [*N*-*methyl*-^{11}C]vorozole ((*S*)-[^{11}C]-4) and *ent*-[*N*-*methyl*-^{11}C]vorozole ((*R*)-[^{11}C]-4)

[*N*-*Methyl*-^{11}C]vorozole ([^{11}C]vorozole, (*S*)-[^{11}C]-**4**) was synthesized by *N*-[^{11}C]methylation of norvorozole ((*S*)-**5**) using $[^{11}C]H_3I$ according to the previously reported procedure.[25] *ent*-[*N*-*Methyl*-^{11}C]vorozole (*ent*-[^{11}C]vorozole, (*R*)-[^{11}C]-**4**) was also synthesized in the same manner using *ent*-norvorozole ((*R*)-**5**). The specific radioactivities of [^{11}C]vorozole ((*S*)-[^{11}C]-**4**) and *ent*-[^{11}C]vorozole ((*R*)-[^{11}C]-**4**) at the end of synthesis were in the range of 13.5–90.7 and 35–42.9 GBq/μmol, respectively, and their radiochemical purities were >99.5%.

4.3. Biology

4.3.1. Animals

Six male adult rhesus monkeys (*Macaca mulatta*; 6.0 ± 0.7 kg) were housed individually under constant temperature and humidity, and were maintained under a 12-h light/dark cycle with free access to water. For PET scans, to four monkeys were administered either [^{11}C]vorozole ((*S*)-[^{11}C]-**4**) or *ent*-[^{11}C]vorozole ((*R*)-[^{11}C]-**4**) and to two monkeys were injected both. Animals were maintained and handled in accordance with the recommendation of the United States National Institutes of Health, and the study was approved by the Animal Care and Use Committee of Kobe Institute at RIKEN (MAH18-05).

4.3.2. PET studies

The monkeys were sedated with ketamine hydrochloride (15 mg/kg, im) and anesthetized continuously with propofol (10 mg/kg/h). A venous cannula was placed in a radial vein. Before the emission scans, transmission scans were performed for 30 min for attenuation correction. [^{11}C]Vorozole ((*S*)-[^{11}C]-**4**) (102–195 MBq) or *ent*-[^{11}C]vorozole ((*R*)-[^{11}C]-**4**) (185–205 MBq) was administered intravenously as a bolus. The monkeys were scanned for 90 min (4 × 30 s, 3 × 60 s, 2 × 150 s, 2 × 300 s, and 7 × 600 s) using a microPET Focus 220 (Siemens, Knoxville, TN, USA).

4.3.3. Analysis of PET data

For quantitative analysis of PET images, kinetic modeling, PMOD software (PMOD Technologies Ltd, Zurich, Switzerland) was employed. Volumes of interest (VOIs) were delineated in the amygdala, hypothalamus, and cerebellum. For each of these regions, decay-corrected time–activity curves were generated. The data were analyzed with a Logan noninvasive model[31] using the time–activity curve of the cerebellum as an input function, and the slope of regression (=distribution volume ratio (DVR) = association rate constant/dissociation rate constant + 1) and binding potential (BP = DVR − 1 = association rate constant/dissociation rate constant) were calculated. Parametric images of DVR were also generated based on pixel-wise kinetic modeling.

Acknowledgments

The authors thank Ms. Masayo Ishikawa at the Center for Advanced Materials Analysis (Suzukakedai), Technical Department, Tokyo Institute of Technology for HRMS analysis, Mr. Masahiro Kurahashi at Sumitomo Heavy Industry Accelerator Service Ltd for operating the cyclotrons, Ms. Emi Hayashinaka and Ms. Chiho Takeda at RIKEN Center for Molecular Imaging Science for supporting the PET scan operation and supporting monkey handling, respectively, and Daicel Chemical Ind., Ltd, Japan for preliminary screening of conditions for optical resolution. This work was partially supported by the Molecular Imaging Program of Research Base for Exploring New Drugs, from the Ministry of Education, Culture, Sports, Science, and Technology (MEXT), Japan.

Supplementary data

Supplementary data (analytical HPLC charts for *rac*-**5**, (*S*)-**5**, and (*R*)-**5** and ^{13}C NMR spectra of *rac*-**5**) associated with this article can be found, in the online version, at doi:10.1016/j.bmc.2010.12.057.

References and notes

1. (a) Hayaishi, O. *Annu. Rev. Biochem.* **1962**, *31*, 25; (b) Mason, H. S. *Annu. Rev. Biochem.* **1965**, *34*, 595.
2. (a) Simpson, E. R.; Mahendroo, M. S.; Means, G. D.; Kilgore, M. W.; Hinshelwood, M. M.; Graham-Lorence, S.; Amarneh, B.; Ito, Y.; Fisher, C. R.; Michael, M. D.; Mendelson, C. R.; Bulun, S. E. *Endocr. Rev.* **1994**, *15*, 342; (b) Santen, R. J.; Brodie, H.; Simpson, E. R.; Siiteri, P. K.; Brodie, A. *Endocr. Rev.* **2009**, *30*, 343.
3. (a) Ryan, K. J. *J. Biol. Chem.* **1959**, *234*, 268; (b) Akhtar, M.; Calder, M. R.; Corina, D. L.; Wright, J. N. *Biochem. J.* **1982**, *201*, 569; (c) Akhtar, M.; Njar, V. C. O.; Wright, J. N. *J. Steroid Biochem. Mol. Biol.* **1993**, *44*, 375.
4. (a) Corbin, C. J.; Graham-Lorence, S.; McPhaul, M.; Mason, J. I.; Mendelson, C. R.; Simpson, E. R. *Proc. Natl. Acad. Sci. U.S.A.* **1988**, *85*, 8948; (b) Terashima, M.; Toda, K.; Kawamoto, T.; Kuribayashi, I.; Ogawa, Y.; Maeda, T.; Shizuta, Y. *Arch. Biochem. Biophys.* **1991**, *285*, 231; (c) Simpson, E. R.; Mahendroo, M. S.; Means, G. D.; Kilgore, M. W.; Corbin, C. J.; Mendelson, C. R. *J. Steroid Biochem. Mol. Biol.* **1993**, *44*, 321.
5. Ghosh, D.; Griswold, J.; Erman, M.; Pangborn, W. *Nature* **2009**, *457*, 219.
6. Grodin, J. M.; Siiteri, P. K.; MacDonald, P. C. *J. Clin. Endocrinol. Metab.* **1973**, *36*, 207.
7. O'Neill, J. S.; Elton, R. A.; Miller, W. R. *Br. Med. J. (Clin. Res. Ed.)* **1988**, *296*, 741.
8. Brueggemeier, R. W.; Hackett, J. C.; Diaz-Cruz, E. S. *Endocr. Rev.* **2005**, *26*, 331.
9. de Jong, P. C.; Blankenstein, M. A.; van de Ven, J.; Nortier, J. W. R.; Blijham, G. H.; Thijssen, J. H. H. *Breast* **2001**, *10*, 91.
10. (a) Riemsma, R.; Forbes, C. A.; Kessels, A.; Lykopoulos, K.; Amonkar, M. M.; Rea, D. W.; Kleijnen, J. *Breast Cancer Res. Treat.* **2010**, *123*, 9; Gibson, L.; Lawrence, D.; Dawson, C.; Bliss, J. *Cochrane Database Syst. Rev.* **2009**. doi:10.1002/14651858.CD003370.pub3; (c) Herold, C. I.; Blackwell, K. L. *Clin. Breast Cancer*

2008, *8*, 50; (d) Eisen, A.; Trudeau, M.; Shelley, W.; Messersmith, H.; Pritchard, K. I. *Cancer Treat. Rev.* **2008**, *34*, 157; (e) Dutta, U.; Pant, K. *Med. Oncol.* **2008**, *25*, 113; (f) Briest, S.; Davidson, N. E. *Rev. Endocr. Metab. Disord.* **2007**, *8*, 215.
11. (a) Giudici, D.; Ornati, G.; Briatico, G.; Buzzetti, F.; Lombardi, P.; di Salle, E. *J. Steroid Biochem.* **1988**, *30*, 391; (b) Deeks, E. D.; Scott, L. J. *Drugs* **2009**, *69*, 889.
12. (a) Plourde, P. V.; Dyroff, M.; Dowsett, M.; Demers, L.; Yates, R.; Webster, A. *J. Steroid Biochem. Mol. Biol.* **1995**, *53*, 175; (b) Sanford, M.; Plosker, G. L. *Drugs* **2008**, *68*, 1319.
13. (a) Bhatnagar, A. S.; Häusler, A.; Schieweck, K.; Lang, M.; Bowman, R. *J. Steroid Biochem. Mol. Biol.* **1990**, *37*, 1021; (b) Bhatnagar, A. S. *Breast Cancer Res. Treat.* **2007**, *105*, S7; (c) Keating, G. M. *Drugs* **2009**, *69*, 1681.
14. (a) Koymans, L. M. H.; Moereels, H.; Bossche, H. V. *J. Steroid Biochem. Mol. Biol.* **1995**, *53*, 191; (b) Graham-Lorence, S.; Amarneh, B.; White, R. E.; Peterson, J. A.; Simpson, E. R. *Protein Sci.* **1995**, *4*, 1065; (c) Kao, Y.-C.; Cam, L. L.; Laughton, C. A.; Zhou, D.; Chen, S. *Cancer Res.* **1996**, *56*, 3451; (d) Chen, S.; Kao, Y.-C.; Laughton, C. A. *J. Steroid Biochem. Mol. Biol.* **1997**, *61*, 107.
15. (a) Goss, P. E.; Strasser, K. *J. Clin. Oncol.* **2001**, *19*, 881; (b) Ingle, J. N. *Clin. Cancer Res.* **2001**, *7*, 4392s; (c) Buzdar, A.; Howell, A. *Clin. Cancer Res.* **2001**, *7*, 2620; (d) Murray, R. *Cancer Chemother. Pharmacol.* **2001**, *48*, 259; (e) Hamilton, A.; Volm, M. *Oncology (Huntingt.)* **2001**, *15*, 965; (f) Buzdar, A. U. *Semin. Oncol.* **2001**, *28*, 291.
16. (a) Lephart, E. D. *Brain Res. Rev.* **1996**, *22*, 1; (b) Roselli, C. F. *J. Steroid Biochem. Mol. Biol.* **2007**, *106*, 143; (c) Garcia-Segura, L. M. *J. Neuroendocrinol.* **2008**, *20*, 705; (d) Roselli, C. E.; Liu, M.; Hurn, P. D. *Semin. Reprod. Med.* **2009**, *27*, 207; (e) Saldanha, C. J.; Duncan, K. A.; Walters, B. J. *Front. Neuroendocrinol.* **2009**, *30*, 106.
17. (a) Compaan, J. C.; Wozniak, A.; De Ruiter, A. J. H.; Koolhaas, J. M.; Hutchison, J. B. *Brain Res. Bull.* **1994**, *35*, 1; (b) Toda, K.; Saibara, T.; Okada, T.; Onishi, S.; Shizuta, Y. *J. Endocrinol.* **2001**, *168*, 217; (c) Goodwin, G. M. *Bipolar Disord.* **2006**, *8*, 516; (d) Trainor, B. C.; Kyomen, H. H.; Marler, C. A. *Front. Neuroendocrinol.* **2006**, *27*, 170.
18. (a) *PET: Molecular Imaging and its Biological Applications*; Phelps, M. E., Ed.; Springer: New York, 2004; (b) Fowler, J. S.; Wolf, A. P. *Acc. Chem. Res.* **1997**, *30*, 181; (c) Schubiger, P. A., Lehmann, L., Friebe, M., Eds. PET Chemistry; Springer: Heidelberg, 2007; (d) Ametamey, S. M.; Honer, M.; Schubiger, P. A. *Chem. Rev.* **2008**, *108*, 1501; (e) Miller, P. W.; Long, N. J.; Vilar, R.; Gee, A. D. *Angew. Chem., Int. Ed.* **2008**, *47*, 8998.
19. Lidström, P.; Bonasera, T. A.; Kirilovas, D.; Lindblom, B.; Lu, L.; Bergström, E.; Bergström, M.; Westlin, J.-E.; Långström, B. *Nucl. Med. Biol.* **1998**, *25*, 497.
20. Wang, M.; Lacy, G.; Gao, M.; Miller, K. D.; Sledge, G. W.; Zheng, Q.-H. *Bioorg. Med. Chem. Lett.* **2007**, *17*, 332.
21. Wang, M.; Mickens, J.; Gao, M.; Miller, K. D.; Sledge, G. W.; Hutchins, G. D.; Zheng, Q.-H. *Steroids* **2009**, *74*, 896.
22. Kil, K.-E.; Biegon, A.; Ding, Y.-S.; Fischer, A.; Ferrieri, R. A.; Kim, S. W.; Pareto, D.; Schueller, M. J.; Fowler, J. S. *Nucl. Med. Biol.* **2009**, *36*, 215.
23. Wouters, W.; Snoeck, E.; De Coster, R. *Breast Cancer Res. Treat.* **1994**, *30*, 89.
24. Vanden Bossche, H. V.; Moereels, H.; Koymans, L. M. *Breast Cancer Res. Treat.* **1994**, *30*, 43.
25. Kim, S. W.; Biegon, A.; Katsamanis, Z. E.; Ehrlich, C. W.; Hooker, J. M.; Shea, C.; Muench, L.; Xu, Y.; King, P.; Carter, P.; Alexoff, D. L.; Fowler, J. S. *Nucl. Med. Biol.* **2009**, *36*, 323.
26. (a) Takahashi, K.; Bergström, M.; Frändberg, P.; Vesström, E.-L.; Watanabe, Y.; Långström, B. *Nucl. Med. Biol.* **2006**, *33*, 599; (b) Takahashi, K.; Hallberg, M.; Magnusson, K.; Nyberg, F.; Watanabe, Y.; Långström, B.; Bergström, M. *NeuroReport* **2007**, *18*, 171; (c) Takahashi, K.; Tamura, Y.; Watanabe, Y.; Långström, B.; Bergström, M. *NeuroReport* **2008**, *19*, 431.
27. Biegon, A.; Kim, S. W.; Alexoff, D. L.; Jayne, M.; Carter, P.; Hubbard, B.; King, P.; Logan, J.; Muench, L.; Pareto, D.; Schlyer, D.; Shea, C.; Telang, F.; Wang, G.-J.; Xu, Y.; Fowler, J. S. *Synapse* **2010**, *64*, 801.
28. (a) Wouters, W.; De Coster, R.; Krekels, M.; van Dun, J.; Beerens, D.; Haelterman, C.; Raeymaekers, A.; Freyne, E.; Van Gelder, J.; Venet, M.; Janssen, P. A. J. *J. Steroid Biochem.* **1989**, *32*, 781; (b) Wouters, W.; De Coster, R.; van Dun, J.; Krekels, M. D. W. G.; Dillen, A.; Raeymaekers, A.; Freyne, E.; Van Gelder, J.; Sanz, G.; Venet, M.; Janssen, M. *J. Steroid Biochem. Mol. Biol.* **1990**, *37*, 1049; (c) Vanden Bossche, H.; Willemsens, G.; Roels, I.; Bellens, D.; Moereels, H.; Coene, M.-C.; le Jeune, L.; Lauwers, W.; Janssen, P. A. J. *Biochem. Pharmacol.* **1990**, *40*, 1707; (d) Wouters, W.; Van Ginckel, R.; Krekels, M.; Bowden, C.; De Coster, R. *J. Steroid Biochem. Mol. Biol.* **1993**, *44*, 617.
29. (a) Willemsens, A. L. A.; Verstappen, W. L. A.; Copmans, A. H.; Vandendriessche, A. M. J.; De Knaep, A. G. M.; Venet, M. G. WO 9411364.; (b) De Knaep, A. G. M.; Vandendriessche, A. M. J.; Daemen, D. J. E.; Dingenen, J. J.; Laenen, K. D.; Nijs, R. L.; Pauwels, F. L. J.; Van den Heuvel, D. F.; Van der Eycken, F. J.; Vanierschot, R. W. E.; van Laar, G. M. L. W.; Verstappen, W. L. A.; Willemsens, B. L. A. *Org. Process Res. Dev.* **2000**, *4*, 162.
30. Långström, B.; Antoni, G.; Gullberg, P.; Halldin, C.; Malmborg, P.; Någren, K.; Rimland, A.; Svärd, H. *J. Nucl. Med.* **1987**, *28*, 1037.
31. Logan, J.; Fowler, J. S.; Volkow, N. D.; Wang, G.-J.; Ding, Y.-S.; Alexoff, D. L. *J. Cereb. Blood Flow Metab.* **1996**, *16*, 834.